J. Fluid Mech. (2012), *vol.* 693, *pp.* 201–215.
doi:10.1017/jfm.2011.510

Three-dimensional Lagrangian Voronoï analysis for clustering of particles and bubbles in turbulence

Yoshiyuki Tagawa[1,3]†, Julián Martínez Mercado[1,3], Vivek N. Prakash[1,3], Enrico Calzavarini[2,3], Chao Sun[1,3]† and Detlef Lohse[1,3]†

[1] Physics of Fluids Group, Faculty of Science and Technology, J.M. Burgers Center for Fluid Dynamics, University of Twente, PO Box 217, 7500 AE Enschede, The Netherlands

[2] Laboratoire de Mécanique de Lille CNRS/UMR 8107, Université Lille 1 and Polytech'Lille, Cité Scientifique Av. P. Langevin, 59650 Villeneuve d'Ascq, France

[3] International Collaboration for Turbulence Research

(Received 21 July 2011; revised 28 September 2011; accepted 14 November 2011; first published online 6 January 2012)

Three-dimensional Voronoï analysis is used to quantify the clustering of inertial particles in homogeneous isotropic turbulence using data sets from numerics in the point particle limit and one experimental data set. We study the clustering behaviour at different density ratios, particle response times (i.e. Stokes numbers St) and two Taylor–Reynolds numbers ($Re_\lambda = 75$ and 180). The probability density functions (p.d.f.s) of the Voronoï cell volumes of light and heavy particles show different behaviour from that of randomly distributed particles, i.e. fluid tracers, implying that clustering is present. The standard deviation of the p.d.f. normalized by that of randomly distributed particles is used to quantify the clustering. The clustering for both light and heavy particles is stronger for higher Re_λ. Light particles show maximum clustering for St around 1–2 for both Taylor–Reynolds numbers. The experimental data set shows reasonable agreement with the numerical results. The results are consistent with previous investigations employing other approaches to quantify the clustering. We also present the joint p.d.f.s of enstrophy and Voronoï volumes and their Lagrangian autocorrelations. The small Voronoï volumes of light particles correspond to regions of higher enstrophy than those of heavy particles, indicating that light particles cluster in higher vorticity regions. The Lagrangian temporal autocorrelation function of Voronoï volumes shows that the clustering of light particles lasts much longer than that of heavy or neutrally buoyant particles. Due to inertial effects arising from the density contrast with the surrounding liquid, light and heavy particles remain clustered for much longer times than the flow structures which cause the clustering.

Key words: homogeneous turbulence, multiphase and particle-laden flows, turbulent flows

† Email addresses for correspondence: y.tagawa@tnw.utwente.nl, c.sun@utwente.nl, d.lohse@utwente.nl

1. Introduction

The distribution of particles transported by turbulent flows is a current research topic with implications in diverse fields, such as process technology (Pratsinis & Vemury 1996), cloud formation (Bodenschatz *et al.* 2010), and plankton dynamics (Schmitt & Seuront 2008). In most of the cases, the particles have a finite size and a different density from the carrier fluid, i.e. they have inertia. These inertial particles cannot completely follow the fluid motion and distribute inhomogeneously within the turbulent flow, leading to clustering or preferential concentration (Toschi & Bodenschatz 2009). The two relevant dimensionless parameters describing the dispersed inertial particles in the fluid are the density ratio $\beta = 3\rho_f/(\rho_f + 2\rho_p)$, where ρ_f and ρ_p are the densities of the carrier fluid and particle, respectively, and the Stokes number, $St = \tau_p/\tau_\eta$, where $\tau_p = a^2/3\beta\nu$ is the particle relaxation time, τ_η is the typical time scale of the flow, which for a turbulent flow is the Kolmogorov time scale, a is the particle radius, and ν is the kinematic viscosity of the fluid.

In recent years, both numerical and experimental studies have quantified the clustering of particles by employing different approaches, such as statistical analysis of single-point measurements (Calzavarini *et al.* 2008*a*), the box-counting method (Fessler, Kulick & Eaton 1994; Aliseda *et al.* 2002), pair correlation functions (Chen, Goto & Vassilicos 2006; Saw *et al.* 2008), the Kaplan–Yorke dimension (Bec *et al.* 2006; Calzavarini *et al.* 2008*c*), Minkowski functionals (Calzavarini *et al.* 2008*c*) and segregation indicators (Calzavarini *et al.* 2008*b*; IJzermans *et al.* 2009). It is not possible to obtain global information on bubble clustering from a single-point analysis (Calzavarini *et al.* 2008*a*). Methods such as box-counting and pair correlation functions, although useful, require the selection of an arbitrary length scale that affects the quantification of the clustering. The Kaplan–Yorke dimension, based on the calculation of the Lyapunov exponents, quantifies the contraction of a dynamical system by considering the separation rates of particle trajectories. Nevertheless, it does not provide global morphological information. Minkowski functionals, originally used to provide complete morphological information of the large-scale distribution of galaxies (Kerscher *et al.* 2001), have been applied to the study of clustering of particles in turbulent flows (Calzavarini *et al.* 2008*c*). Calzavarini *et al.* (2008*c*) found that light particles cluster in filamentary structures, whereas heavy particles have a wall-like topology around interconnected tunnels, and obviously no clustering was observed for neutrally buoyant tracers. In the above numerical simulations and experiments, the strongest clustering was found for particles with $St \approx O(1)$. The problem with Minkowski-type analysis is that it is numerically expensive, and it does not provide information on the Lagrangian evolution of the clusters.

An alternative mathematical tool that can be used to study clustering is the Voronoï tessellation, which has been used in astronomy as a tool to characterize clustering of galaxies (van de Weygaert & Icke 1989). Recently, Monchaux, Bourgoin & Cartellier (2010) have applied a Voronoï analysis to quantify the clustering of heavy particles in grid-generated turbulence. This Voronoï approach does not require the selection of an arbitrary length scale for a fixed particle number, and it can provide information on the Lagrangian statistics of clustering (Monchaux *et al.* 2010). Monchaux *et al.* (2010) have obtained two-dimensional particle positions by imaging a turbulent flow in a wind tunnel seeded with droplets. The Voronoï cells are defined based on the positions of the particles within the measurement domain. One can quantify the clustering by calculating the probability density function (p.d.f.) of the normalized areas of the Voronoï cells. The p.d.f. will have a different shape for inertial particles when compared to the corresponding p.d.f. of randomly distributed particles. The main

	N	Re_λ	η	τ_η	$N_{particles}$	St
Simulation A	128	75	0.0332	0.1104	1.0×10^3	0.1–4.0
Simulation B	512	180	0.001	0.0483	6.4×10^4	0.1–4.1
Experiment	—	162	288 μm	80 ms	1.3×10^3	0.04 ± 0.02

TABLE 1. Summary of the simulation and experimental parameters, where N is the size of the numerical domain, Re_λ is the Taylor–Reynolds number, η, τ_η are the Kolmogorov length and time scales, respectively, and $N_{particles}$ is the number of particles in the simulations, and the time-averaged particle number in the measurement volume for the experiment. St is the Stokes number.

difference is observed at the small and large values of normalized areas, where the p.d.f. of heavy particles has a higher probability than for randomly distributed particles. There is a central region where there is no significant difference between the p.d.f.s of heavy particles and randomly distributed ones. The values of normalized areas at which the p.d.f. deviates from the randomly distributed particles can be used as thresholds to classify Voronoï cells that belong to either clusters or voids. Monchaux *et al.* (2010) report a maximum preferential concentration for St around unity, in agreement with other methods that have been used to study clustering.

The objective of the present work is to extend the work of Monchaux *et al.* (2010) to (i) three dimensions, and (ii) a much larger range of density ratios (including light, heavy, and neutrally buoyant particles) and Stokes numbers, i.e. we quantify particle clustering by applying three-dimensional Voronoï analysis to both numerical and experimental data sets of particles and bubbles. Moreover, we (iii) correlate the clustering behaviour of different particles with local turbulent flow quantities, and (iv) study the Lagrangian temporal evolution of the clusters.

2. Experimental and numerical data sets and Voronoï analysis

2.1. *Data sets*

The numerical scheme for a dilute suspension (neglecting particle collisions) of point particles in homogeneous and isotropic turbulence is described as follows (Maxey & Riley 1983; Calzavarini *et al.* 2008*c*):

$$\frac{\mathrm{d}\boldsymbol{v}}{\mathrm{d}t} = \beta \frac{\mathrm{D}}{\mathrm{D}t}\boldsymbol{u}(\boldsymbol{x}(t), t) - \frac{1}{\tau_p}(\boldsymbol{v} - \boldsymbol{u}(\boldsymbol{x}(t), t)), \tag{2.1}$$

where $\boldsymbol{v} = \mathrm{d}\boldsymbol{x}/\mathrm{d}t$ is the particle velocity and $\boldsymbol{u}(\boldsymbol{x}(t), t)$ the velocity field. The dimensionless numbers used to model the particle motion are the density difference between the particle and the fluid β and the Stokes number St. The values of $\beta = 0, 1$ and 3 correspond to very heavy particles, neutrally buoyant tracers, and very light particles (bubbles in water), respectively. When $St = 0$, the particles perfectly follow the fluid flow behaving as fluid tracers. As summarized in table 1, we explore a parameter space of $\beta = 0, 1$ and 3 and St ranging from 0.1 to 4.0 consisting of 24 values at $Re_\lambda = 75$ with the spatial resolution of $N = 128^3$. For $Re_\lambda = 180$ with $N = 512^3$, we study five different values of $St = 0.1, 0.6, 1.6, 2.6$, and 4.1 (from iCFDdatabase http://cfd.cineca.it; Calzavarini *et al.* 2008*c*). The simulation of the Navier–Stokes equation is based on a 2/3 de-aliased pseudo-spectral algorithm with second-order Adams–Bashforth time-stepping (for details see Bec *et al.* 2006).

Simulations were performed in a cubic box of side $L = 2\pi$ with periodic boundary conditions. The forcing adopted acts only at the largest scale; it is implemented by keeping constant the kinetic energy content of the smallest shell ($|k| \leqslant 1$) in Fourier space. The intensity of the forcing is adjusted in such a way as to have a turbulent dissipative scale (η) of about 0.8 lattice grids in real space. Particle dynamics is evolved with time steps $O(10)$ times smaller than the smallest Stokes time, leading to an accurate resolution of the particle trajectories. Tri-linear interpolation is used to determine the value of the velocity field at the particle position. The numerical code was also validated by comparison with an independent code implementing different temporal integration scheme, different particle interpolation and different large-scale forcing (Toschi *et al.* 2009). The simulations extend over a few $O(1)$ large-eddy-turnover times, which is enough for particles to reach a statistically steady distribution. In the present analysis, we fix the number of particles ($N_{particles}$) for given Reynolds numbers: 1000 particles for the simulation with the domain size of 128^3 at $Re_\lambda = 75$, and 6.4×10^4 particles for the simulation of 512^3 at $Re_\lambda = 180$. The number of particles normalized by the corresponding domain volume, i.e. the volume concentrations of the particles, for the two Re_λ are identical. In one particular case of $Re_\lambda = 75$ and $St = 0.6$, the particle number is varied from 100 to 1×10^5.

We conduct experiments in the Twente Water Tunnel (TWT), an 8 m long vertical water tunnel designed for studying two-phase flows. By means of an active grid, nearly homogeneous and isotropic turbulence with Re_λ up to 300 can be achieved. A measurement section with dimensions 2 m $\times$ 0.45 m $\times$ 0.45 m with three glass walls provides optical access for three-dimensional particle tracking velocimetry (PTV) system. Micro-bubbles with a mean radius of 170 ± 60 μm are generated by blowing pressurized air through a ceramic porous plate that is located in the upper part of the water tunnel. These micro-bubbles are advected downwards by the flow passing through the measurement section. In our three-dimensional particle tracking velocimetry (3D-PTV) micro-bubble experiments, we use a four-camera system to get micro-bubble positions in the active-grid-generated turbulence in the TWT. The experimental data are collected for a duration of 6 s (three times the large eddy turnover time) at an acquisition rate of 1000 frames s^{-1}. For the experimental data, $Re_\lambda = 162$, $\beta = 3$ and $St = 0.04 \pm 0.02$, and the time-averaged number of particles inside the measurement volume of 70 mm $\times$ 70 mm $\times$ 70 mm is 1.3×10^3 (for further details, see Martinez Mercado *et al.* 2010, 2011).

2.2. *Voronoï analysis*

The Voronoï diagram is a spatial tessellation where each Voronoï cell is defined at the particle location based on the distance to the neighbouring particles (Okabe *et al.* 2000). Every point in a Voronoï cell is closest to the particle position compared to the neighbouring particles, the exceptions being the vertices, borderlines and facets (see figure 1). Therefore, in regions where particles cluster, the volume of the Voronoï cells is smaller than that of the cells in neighbouring regions. Hence, the volume of the Voronoï cells is inversely proportional to the local particle concentration. The p.d.f. of the Voronoï volumes normalized by the mean volume for randomly distributed particles can be well described by a Γ-distribution (Ferenc & Néda 2007) (see figure 2). In the three-dimensional case, the Γ-distribution has the following prefactor and exponent:

$$f(x) = \frac{3125}{24} x^4 \exp(-5x). \tag{2.2}$$

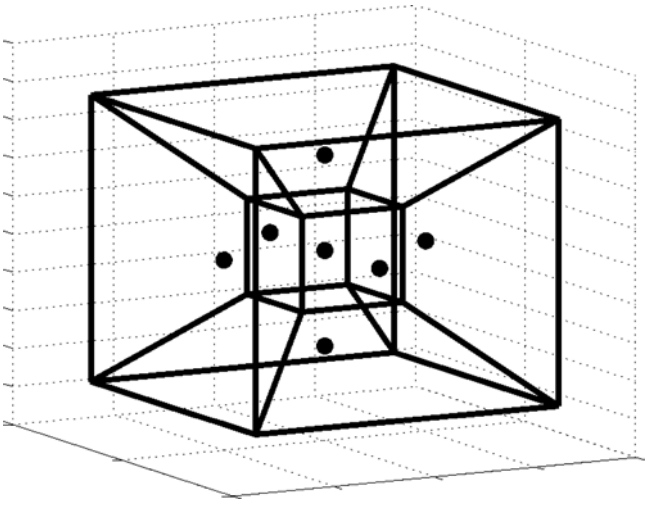

FIGURE 1. An example of a three-dimensional Voronoï tessellation. The dots represent particle positions and lines represent the borders of the Voronoï cells.

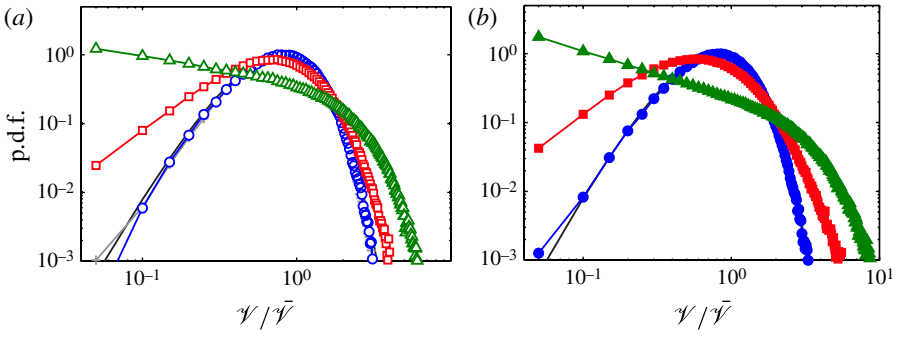

FIGURE 2. (Colour online available at journals.cambridge.org/flm) The normalized Voronoï volume p.d.f.s for heavy (squares), neutrally buoyant (circles), and light particles (triangles) at $St = 0.6$ from direct numerical simulation (DNS) at (*a*) $Re_\lambda = 75$ and (*b*) $Re_\lambda = 180$. The thick line shows the Γ-distribution (2.2) for randomly distributed particles (Ferenc & Néda 2007); the p.d.f. of the neutrally buoyant particles agrees well with the randomly distributed particles (+). Both heavy and light particles show clustering, but light particles show the maximum clustering.

Here x is the Voronoï volume normalized by the mean volume. Particles which are not randomly distributed will have a p.d.f. that deviates from this Γ-distribution, indicating preferential concentration. The Voronoï cells of particles located near the edges of the domain are ill-defined, i.e. they either do not close or close at points outside the domain. These cells at the border of the domain are not considered for the analysis.

3. Results

First, we present results on the effect of the density ratio (β) on the clustering, followed by the effect of the Stokes number (St) and the number of particles ($N_{particles}$). Then, we show how the volume of Voronoï cells ($\mathscr{V}$) and enstrophy are related.

Finally, we present results on the Lagrangian autocorrelations of Voronoï volumes and enstrophy.

3.1. *Density effect*

Here we study the clustering behaviour of particles of different β at a fixed St for two different Re_λ. Figure 2 shows the p.d.f.s of the Voronoï volumes ($\mathscr{V}$) normalized by their averaged volume ($\bar{\mathscr{V}}$), $\mathscr{V}/\bar{\mathscr{V}}$, for heavy, neutrally buoyant, and light particles of $St = 0.6$ at $Re_\lambda = 75$ (figure 2*a*) and 180 (figure 2*b*). It clearly shows that the trends in the probability density functions are similar for both Re_λ. The p.d.f. of neutrally buoyant particles follows the Γ-distribution (2.2) quite well, reflecting that neutrally buoyant particles do not have any preferential concentration. In contrast, the p.d.f.s of light and heavy particles clearly show different behaviour compared to the randomly distributed particles. We observe that the probability of finding either small or large Voronoï volumes is higher for both light and heavy particles. The two regions of small and large volumes can be used to identify clusters and voids. The strongest clustering is observed for light particles, as the probability of finding small Voronoï volumes is the highest. Owing to the density difference, light particles accumulate in vortex filaments due to centrifugal forces (Mazzitelli, Lohse & Toschi 2003; Mazzitelli & Lohse 2004; Biferale, Scagliarini & Toschi 2010), while heavy particles concentrate in regions of intense strain (Bec *et al.* 2006). Here, although the heavy particles show clustering, it is less compared to light particles. These results are consistent with the Minkowski analysis by Calzavarini *et al.* (2008*c*).

3.2. *Stokes number effect*

In this section, we study the effect of St on the clustering behaviour for the three types of particles. We study the clustering behaviour of the particles by examining the deviations of their Voronoï volume p.d.f.s from the Γ-distribution.

Figure 3 shows p.d.f.s of light ($\beta = 3$) and heavy ($\beta = 0$) particles for different St at Re_λ of 75 and 180. First, we discuss the clustering of light particles as shown in figure 3 for Re_λ of (*a*) 75 and (*b*) 180. Both Reynolds numbers give a similar trend with increasing St. When St increases, the probability of finding clusters and voids increases up to a value of $St = 1.6$, after which the dependence becomes weaker for both Re_λ. We note that the experimental result, shown with stars in figure 3(*b*), for micro-bubbles with $St = 0.04 \pm 0.02$ agrees reasonably well with the trend of the numerical data for light particles. In any case, for these small Stokes numbers, the p.d.f. of the Voronoï volumes is still qualitatively similar to that of tracers. Another important feature of the light particle p.d.f. is that the highest probability occurs at the smallest volume and decreases monotonically with increasing volume for St in the range of 0.6 to 4. As studied by Calzavarini *et al.* (2008*c*), bubbles in this range of St tend to get trapped in vortex filaments, leaving void regions. Thus, most of the bubbles are concentrated in small regions and there are few bubbles outside these small regions.

In general, the clustering of heavy particles is weaker than that of light particles. For heavy particles, as shown in figure 3(*c,d*), as St increases, the probability of finding clusters and voids increases up to a value of $St = 1.6$; then the St dependence changes for different Re_λ, as discussed below.

Monchaux *et al.* (2010) found that the Voronoï area statistics of heavy particles can be well fitted by a log-normal distribution. For comparison, figure 4(*a*) shows the log-normal fitting for the p.d.f.s of the present three-dimensional Voronoï volumes for the three different types of particles. It is clear that the Voronoï volume statistics

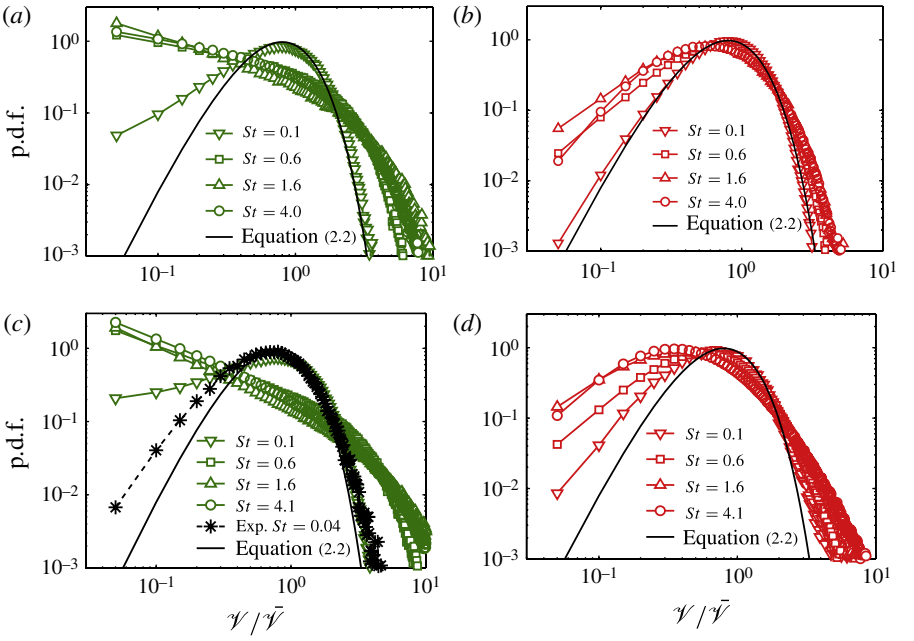

FIGURE 3. (Colour online) The normalized Voronoï volume p.d.f.s for different St ranging from 0.1 to 4 in the numerics for (*a*) light particles $\beta = 3$ at $Re_\lambda = 75$, (*b*) light particles $\beta = 3$ at $Re_\lambda = 180$, (*c*) heavy particles $\beta = 0$ at $Re_\lambda = 75$, and (*d*) heavy particles $\beta = 0$ at $Re_\lambda = 180$. The stars in (*b*) correspond to the experimental result with $St = 0.04 \pm 0.02$ at $Re_\lambda = 162$.

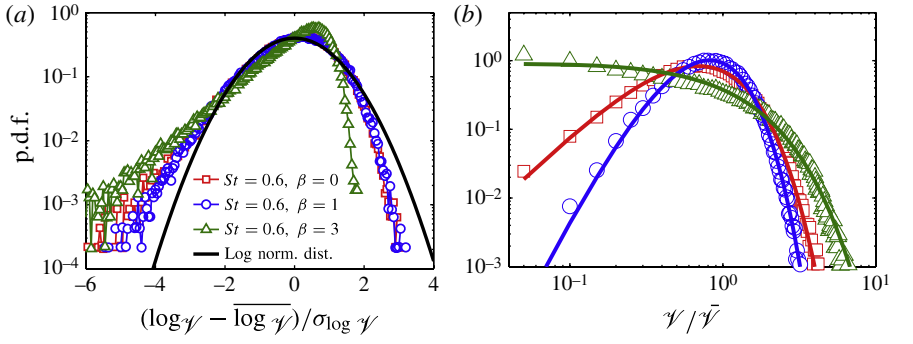

FIGURE 4. (Colour online) The comparison between log-normal and Γ-distribution of (3.1) fitting for the p.d.f. of the three-dimensional Voronoï volumes. Open symbols represent heavy (squares), neutrally buoyant (circles), and light particles (triangles) at $St = 0.6$ from DNS at $Re_\lambda = 75$; the lines represent (*a*) log-normal, and (*b*) Γ-distribution.

cannot be characterized well by the log-normal function, not even for the neutrally buoyant particles. However, the p.d.f.s for all types of particles can be fitted very well by the Γ-distribution (see figure 4*b*) with only one fitting parameter σ:

$$f(x) = \frac{1}{\sigma^{(2/\sigma^2)}\Gamma\left(\dfrac{1}{\sigma^2}\right)} x^{(1/\sigma^2)-1}\exp^{-(x/\sigma^2)}, \tag{3.1}$$

where σ is the standard deviation of the Voronoï volumes. Hence σ provides a proper statistical quantification of Voronoï volumes.

In order to quantify the clustering using a single number, we use the standard deviation σ of the normalized Voronoï volume distributions. In figure 5(*a*), we plot σ normalized by the standard deviation of the Voronoï volumes for randomly distributed particles σ_Γ. The magnitude of the indicator σ/σ_Γ distinguishes the behaviour of light, neutrally buoyant, and heavy particles. A higher value of the indicator reflects stronger clustering for a given Re_λ. For neutrally buoyant particles there is no observed clustering, hence the indicator value is constant at 1. Heavy particles show clustering and the indicator value saturates at $St \approx 1$–2 at $Re_\lambda = 75$. However, the indicator value continuously increases with St at the higher Reynolds number of $Re_\lambda = 180$, and the absolute value of the indicator σ/σ_Γ is larger for higher Re_λ. This indicates that the clustering of heavy particles is stronger at higher Re_λ for a given St. Figure 5(*a*) shows that the absolute value of the indicator σ/σ_Γ for light particles is also larger for higher Re_λ, revealing a stronger clustering for light particles at higher Re_λ. The reason for the Reynolds number effect could be because of the changing range of length scales of the vortex filaments which affect the clustering. At higher Re_λ, there is a wider range of clustering length scales, resulting in a Voronoï volume distribution with a higher value of standard deviation. The curves corresponding to light particles show the strongest clustering, with a peak at $St \approx 1$–2 for both $Re_\lambda = 75$ and 180. This clustering result has a consistent trend with that of the Kaplan–Yorke analysis (Calzavarini *et al.* 2008*c*).

We also add the data point for the standard deviation of the experimental Voronoï volume p.d.f. as shown in figure 5. Although the mean value of the indicator σ/σ_Γ for the experimental data is higher than those from the numerical simulations of light point particles, there is good agreement with the numerical trend within the experimental error bar. More experimental data at larger Stokes numbers, i.e. larger bubbles, will be needed to come to a final conclusion on this issue.

3.3. *Effects of the number of particles*

In principle, one can expect different behaviours depending on the number density of particles. In the simulation data set A, there are 10^5 particles available for one special case of $Re_\lambda = 75$ and $St = 0.6$. Using this snapshot, we study the effects of the particle number on the value of the clustering indicator σ/σ_Γ. We subsample data from this snapshot by selecting the required number particles and computing the Voronoï statistics. This subsampling procedure is randomized and then carried out at least 100 times for each case of particle number. Figure 6 shows the effect of varying the number of particles on the clustering indicator σ/σ_Γ and the error bars represent the standard deviation of all the subsamples of a given number of particles. In the present data set, the mean distances of particles are 34.47η for $N_{particles} = 10^2$, 6η for $N_{particles} = 10^3$, 3.44η for $N_{particles} = 10^5$, which are all above 1η. Hence, we are always studying situations where the mean particle distances are in the inertial range.

As shown in figure 6, for light and heavy particles the value of the indicator increases as the number of the particles is increased. The evolution of the value of the indicator σ/σ_Γ is steeper with increasing number of particles, and there seems to be no plateau region where the indicator value saturates. We do not understand the exact reason for this particle number dependence. One possible reason could be that the clusters have a complicated structure (Calzavarini *et al.* 2008*c*). However, for a given number of particles, the indicator does show a consistent trend: a stronger clustering for light particles, weaker clustering for heavy particles, and no clustering for neutrally

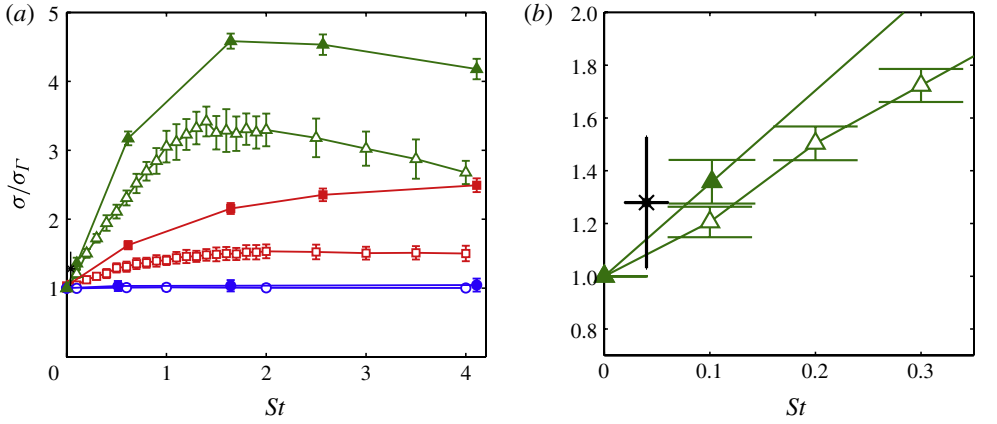

FIGURE 5. (Colour online) (*a*) Normalized standard deviation σ/σ_Γ (indicator) of the Voronoï volume distributions versus St for the two different Re_λ from DNS data. The symbols correspond to heavy (squares), neutrally buoyant (circles), and light particles (triangles). Open and filled symbols represent data at $Re_\lambda = 75$ and $Re_\lambda = 180$, respectively. The value of the indicator for neutrally buoyant particles remains constant at 1, i.e. clustering is not observed, whereas light particles show the most clustering with a peak at $St \approx 1.5$ for both Re_λ. The experimental result of micro-bubbles is plotted with the star. (*b*) An enlarged plot showing only the results for light particles.

buoyant particles. Moreover, the error of the indicator calculated at $N_{particle} = 1000$ is less than 4 %. Therefore, at a fixed number of particles, the clustering indicator σ/σ_Γ of the Voronoï volume is robust. In the analysis that follows, we use the data of $N_{particles} = 1000$ for the simulation with the domain size of $N = 128^3$ at $Re_\lambda = 75$ (simulation A).

3.4. *Relation between the volume of the Voronoï cell and enstrophy*

We relate the Voronoï volumes for the three different types of particles with turbulent flow quantities. A natural property for this comparison would be the enstrophy $\Omega = \omega^2/2$ (where ω is vorticity). Benzi *et al.* (2009) have shown that different types of particles react sensitively to the local enstrophy at the particle position, reflecting their tendency to stay in regions with different vorticity contents. We thus calculate the joint p.d.f. of Voronoï volumes and enstrophy for three types of particles at a fixed $St = 0.6$ for $Re_\lambda = 75$. For comparison, we also calculate the joint p.d.f. for the case of neutrally buoyant particles with the smallest St available in the simulations ($St = 0.1$ and $\beta = 1$). The statistical behaviour of these particles is expected to be close to that of ideal fluid tracers ($St = 0$ and $\beta = 1$). From now on, we refer to this case as the fluid tracer case. The Voronoï volume and the enstrophy are normalized by the mean values ($\mathcal{V}_{tr}$ and Ω_{tr}) of the fluid tracers. Figure 7 shows the joint p.d.f.s of the normalized Voronoï volume ($\mathcal{V}/\mathcal{V}_{tr}$) and the normalized enstrophy (Ω/Ω_{tr}) for the different types of particles. The joint p.d.f. for neutrally buoyant particles of $St = 0.6$, shown in figure 7(*c*), is very similar to that of fluid tracers shown in figure 7(*a*). We observe a clear difference in the joint p.d.f. for heavy and light particles, as shown in figure 7(*b,d*). The coordinates corresponding to the peak of the joint p.d.f. $((\Omega/\Omega_{tr})^{max}_{jpdf}, (\mathcal{V}^p/\mathcal{V}_{tr})^{max}_{jpdf})$ is indicated by the crosses in the figure for each case. Compared to the tracer case, a slightly lower $(\mathcal{V}^p/\mathcal{V}_{tr})^{max}_{jpdf}$ and a lower $(\Omega/\Omega_{tr})^{max}_{jpdf}$ for heavy particles indicates more clustering at low enstrophy regions. The maximum

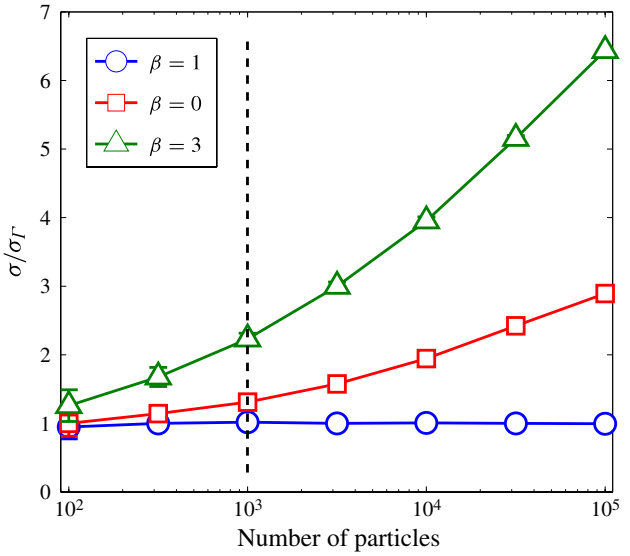

FIGURE 6. (Colour online) Normalized standard deviation of the Voronoï volume distributions as a function of number of particles taken from a snapshot case at $Re_\lambda = 75$. The dashed line shows the number of particles we used in the present work at $Re_\lambda = 75$ and $St = 0.6$ (simulation A).

value of the joint p.d.f.s for the light particles is located at the region with a much higher enstrophy and a smaller Voronoï volume. This shows that the light particles shows strong clustering at high enstrophy regions.

The St dependence on the peak coordinates of the joint p.d.f. $((\Omega/\Omega_{tr})^{max}_{jpdf}, (\mathscr{V}^p/\mathscr{V}_{tr})^{max}_{jpdf})$ is plotted in figure 8. As shown in figure 8(a), the value of $(\mathscr{V}^p/\mathscr{V}_{tr})^{max}_{jpdf}$ for neutrally buoyant particles is nearly same as that of tracers at St from 0.1 to 4. The value of $(\mathscr{V}^p/\mathscr{V}_{tr})^{max}_{jpdf}$ for heavy particles is slightly smaller than unity for all St, indicating clustering. Figure 8(a) also shows that the clustering for light particles is stronger, as evidenced by the much smaller $(\mathscr{V}^p/\mathscr{V}_{tr})^{max}_{jpdf}$ compared to those of neutrally buoyant and heavy particles at all St. The minimum value of $(\mathscr{V}^p/\mathscr{V}_{tr})^{max}_{jpdf}$ indicating strongest clustering for the light particles is located at $St = 1$–2, which is in excellent agreement with the results obtained using the indicator σ/σ_Γ (figure 5). The corresponding enstrophy at the peak $((\Omega/\Omega_{tr})^{max}_{jpdf})$ of the joint p.d.f. versus St for the different particles is shown in figure 8(b). The value of $(\Omega/\Omega_{tr})^{max}_{jpdf}$ for the heavy particles is smaller than unity, and it is much larger than unity for the light particles. This reflects the clustering of light particles in flow regions with very high enstrophy, whereas heavy particles cluster in low enstrophy regions for all St in the present study.

3.5. *Voronoï Lagrangian autocorrelation*

Finally, we conduct a Lagrangian analysis on the Voronoï volumes. For each type of particle we calculate the Lagrangian autocorrelation of its associated Voronoï volume. Figure 9(a) shows a typical temporal evolution of Voronoï volumes for the three types of particles at $St = 0.6$ and $Re_\lambda = 75$. To compare the behaviour of the three different particles, we choose particles with similar Voronoï volume at the starting time and trace their time evolution. While the Voronoï volumes of heavy and neutrally buoyant particles change frequently in time, it is clearly seen that light particles tend

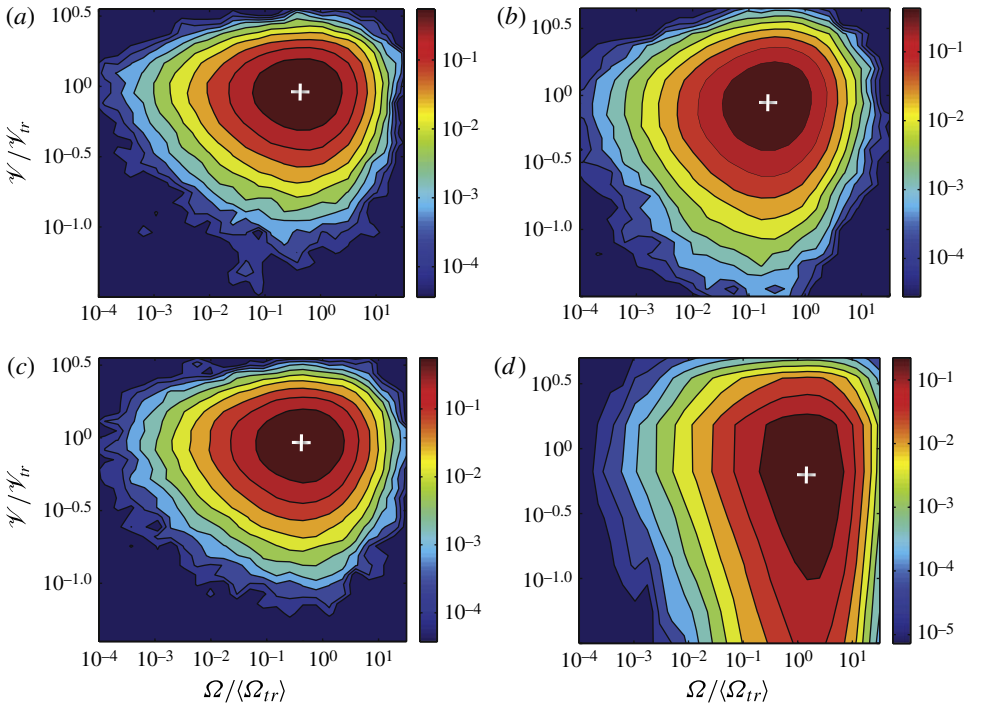

FIGURE 7. (Colour online) Joint p.d.f.s of normalized Voronoï volumes and enstrophy for tracers and particles at $St = 0.6$ for $Re_\lambda = 75$: (*a*) fluid tracers, (*b*) heavy particles, (*c*) neutrally buoyant particles, and (*d*) light particles. The cross indicates the location of the maximum probability (peak) for each case. (*a*) Tracers, (*b*) $\beta = 0$, $St = 0.6$, (*c*) $\beta = 1$, $St = 0.6$, (*d*) $\beta = 3$, $St = 0.6$.

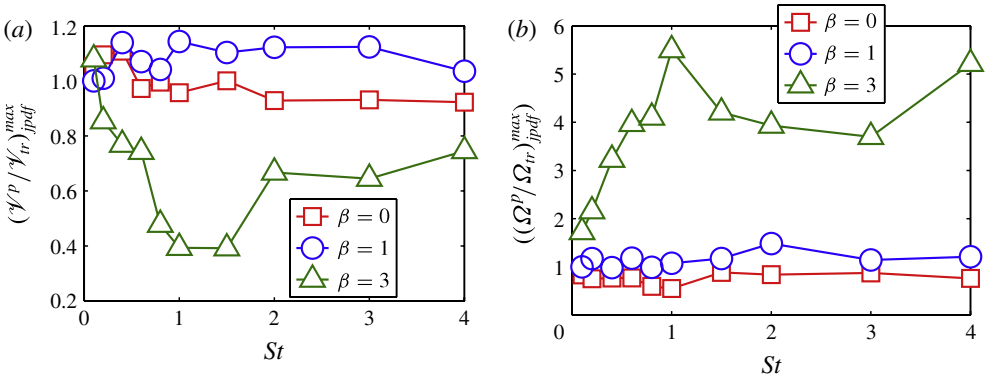

FIGURE 8. (Colour online) The coordinates of the peak of the joint p.d.f.s of normalized Voronoï volumes and enstrophy as a function of St: (*a*) $\mathscr{V}^p/\mathscr{V}_{tr}$ versus St, (*b*) Ω^p/Ω_{tr} versus St.

to have small values for longer times. This suggests that light particles are trapped in clustered regions for a long time and are suddenly ejected, as seen in figure 9(*a*) around $\tau/\tau_\eta \approx 95$.

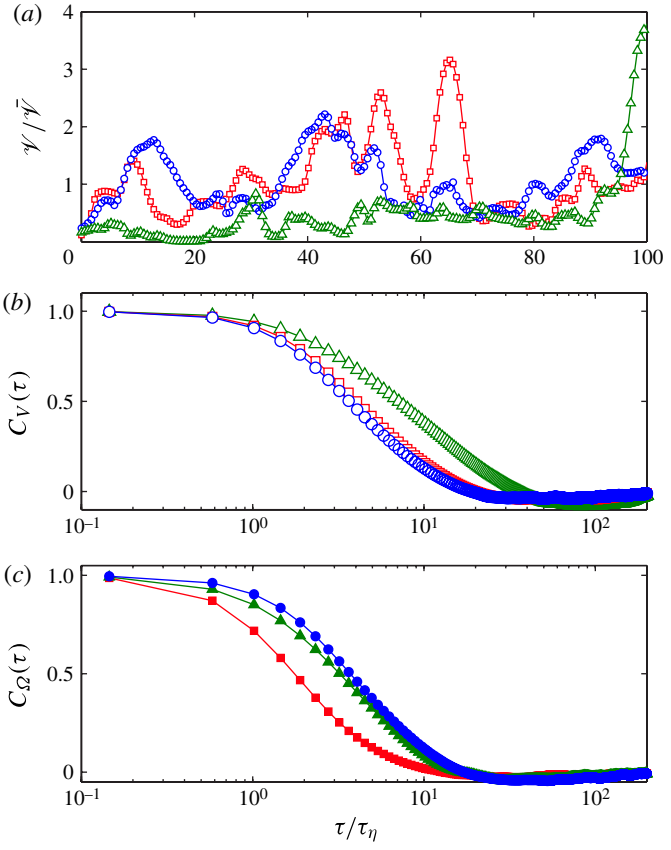

FIGURE 9. (Colour online) Lagrangian Voronoï analysis for heavy (squares), neutrally buoyant (circles), and light particles (triangles) at $St = 0.6$ and $Re_\lambda = 75$. (*a*) Temporal evolution of Voronoï volumes. (*b*) Temporal autocorrelation functions of Voronoï volumes. (*c*) Temporal autocorrelation functions of enstrophy.

Figure 9(*b*) shows the autocorrelation function $C_V(\tau)$ for heavy, neutrally buoyant, and light particles at a fixed $St = 0.6$ and $Re_\lambda = 75$. We define the decorrelation time τ_V as the time when the autocorrelation function has decreased to 1/2, i.e. $C_V(\tau_V) = 1/2$. As shown in figure 9(*b*), the decorrelation time for light particles is around $\tau_V \sim 7\tau_\eta$, whereas for heavy and neutrally buoyant particles decorrelation already occurs around $4\tau_\eta$. Thus the clustering of light particles lasts for a longer time as compared to heavy and neutrally buoyant particles. As shown by Calzavarini *et al.* (2008*c*), light particles accumulate in filamentary structures and heavy ones tend to cluster outside these structures to form wall-like interconnected tunnels. These differences in the morphology of the clustered particles could be a possible reason for the light particles being clustered for a longer time as compared to heavy particles.

We also compare the autocorrelation time scale of the Voronoï volumes to that of the enstrophy shown in figure 9(*c*) for the same St and Re_λ. First, as expected, for neutrally buoyant particles, the Lagrangian decorrelation time for the Voronoï volumes is comparable to that of the enstrophy (τ_Ω), i.e. $\tau_\Omega \sim \tau_V \sim 4\tau_\eta$, because the neutrally buoyant particles do not cluster. However, remarkably, for light particles the decorrelation time of the Voronoï volumes is much larger, $\tau_V \sim 7\tau_\eta$, i.e. more than

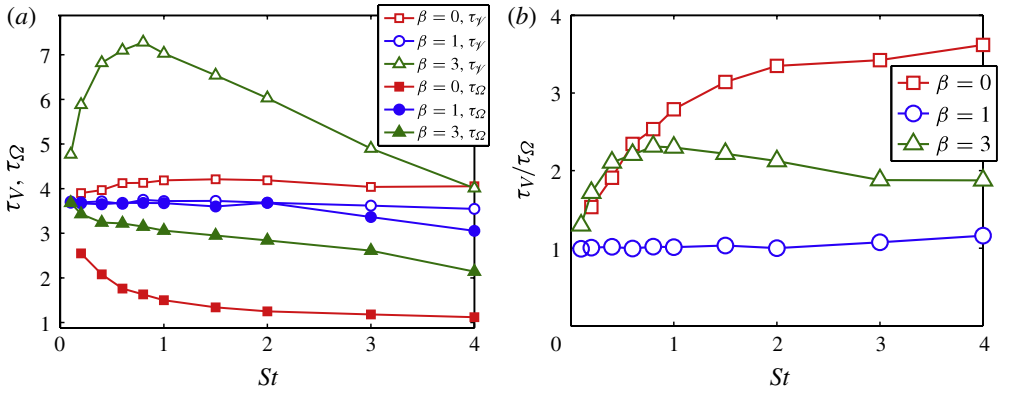

FIGURE 10. (Colour online) (*a*) Decorrelation time of Voronoï volume (τ_V) and enstrophy (τ_Ω) as a function of St at $Re_\lambda = 75$ for heavy (squares), neutrally buoyant (circles), and light particles (triangles). Open and filled symbols represent decorrelation times of Voronoï volume and enstrophy, respectively. (*b*) The ratio of decorrelation times (τ_V/τ_Ω) as a function of St.

twice as large as the autocorrelation time scale $\tau_\Omega \sim 3\tau_\eta$ of the enstrophy itself. For heavy particles, the Lagrangian decorrelation time of the Voronoï volumes is around $\tau_V \sim 4\tau_\eta$, which is also about twice that of enstrophy $\tau_\Omega \sim 2\tau_\eta$.

We also study the St dependence of the decorrelation time scales of Voronoï volume (τ_V) and enstrophy (τ_Ω) at $Re_\lambda = 75$ for heavy, neutrally buoyant, and light particles as shown in figure 10(*a*). We observe that τ_V for light particles is always larger than heavy and neutrally buoyant particles in the St range 0.1 to 4, with a peak around $St = 1$. This suggests that the light particles cluster for a longer time in the range of St studied.

It is well known that flow regions of high enstrophy trap bubbles and regions with intense strain accumulate heavy particles. Figure 10(*a*) also shows that τ_V for both light and heavy particles is much larger than their decorrelation time of enstrophy τ_Ω for all St from 0.1 to 4. This is more clearly seen in figure 10(*b*), where the ratio τ_V/τ_Ω for both light and heavy particles is greater than unity for all St, while this ratio is always close to unity for the neutrally buoyant particles. Remarkably, this means that the lifetimes of the clustered bubbles and heavy particles are much longer than the lifetime of the trapping flow structures themselves. The interpretation is that clustered particles are constrained in different regions of the flow and due to their inertia need time to reorganize themselves in the flow after sudden changes in flow conditions. However, neutrally buoyant particles do not have this constraint and are distributed more evenly at any given time in the flow. Figure 10(*b*) shows that the ratio τ_V/τ_Ω for light particles has a weakly decreasing trend at St larger than unity. The ratio τ_V/τ_Ω for heavy particles monotonically increases with increasing St, and it is larger compared to light particles for $St > 0.5$.

4. Conclusion

We use three-dimensional Voronoï analysis to study particle clustering in homogeneous isotropic turbulence with both numerical data in the point particle limit and one experimental data set. The analysis is applied to inertial particles (light, neutrally buoyant, and heavy) of different density ratios β, St ranging from 0.1 to 4 and two different Taylor–Reynolds numbers ($Re_\lambda = 75$ and 180). In the entire range

of parameters covered, the Voronoï volume p.d.f.s of neutrally buoyant particles agree well with the Γ-distribution for randomly distributed particles. At a fixed value of St, the p.d.f.s of Voronoï volumes of light and heavy particles show higher probability of having small and large Voronoï volumes than randomly distributed particles, reflecting the clustering behaviour. The standard deviation of normalized Voronoï volumes σ/σ_Γ is used as an indicator to quantify the clustering. Heavy particles show some clustering, and light particles have a much stronger clustering. Both heavy and light particles show a stronger clustering for higher Re_λ. The maximum clustering for light particles is around $St \approx 1$–2 for both Taylor–Reynolds numbers, and this maximum clustering range has a consistent trend with that of the Kaplan–Yorke analysis. We check the effect of number of particles on the value of the indicator and find that the clustering trend is robust for a given number of particles.

For one (small) Stokes number $St = 0.04 \pm 0.02$ we have also extracted the three-dimensional Voronoï volume p.d.f. from experimental data. Though the p.d.f. fits into the general trend – at these small Stokes numbers the p.d.f. nearly follows a Γ-distribution – a quantitative analysis shows that the experimental p.d.f. of three-dimensional Voronoï volumes is slightly broader than that obtained from point–particle simulations. More experiments with larger Stokes numbers will have to be done to judge whether this is a limitation of the point–particle approach, a consequence of the neglect of two-way and four-way coupling in the numerics, or whether the experimental data are not precise enough. From our point of view, the Voronoï analysis is an excellent means to quantitatively compare clustering effects of particles in experimental and numerical data sets.

Finally, we show that the Voronoï analysis can be connected to local flow properties such as enstrophy. By comparing the joint p.d.f.s of enstrophy and Voronoï volumes and their Lagrangian autocorrelation, the clustering behaviour of heavy, neutrally buoyant, and light particles can be further distinguished. It is found that the light particles strongly cluster in flow regions with very high enstrophy, whereas heavy particles weakly cluster in low enstrophy regions for all St in the present study. From the Lagrangian autocorrelation of Voronoï volumes we conclude that the clustering of light particles lasts much longer than that of heavy or neutrally buoyant particles. And because of inertial effects due to the density difference from the carrying fluid, light and heavy particles remain clustered for a much longer time than the flow structures themselves.

Acknowledgements

We would like to acknowledge the support from COST Action MP0806: *Particles in Turbulence*. We acknowledge M. Bourgoin, R. Monchaux, S. G. Huisman, C. Sanli, D. van der Meer, and F. Toschi for useful discussions. J.M.M. acknowledges the foundation for Fundamental Research of Matter (FOM) for the funding within the Industrial Partnership Programme: *Fundamentals of Heterogeneous Bubbly Flows*.

REFERENCES

ALISEDA, A., CARTELLIER, A., HAINAUX, F. & LASHERAS, J. C. 2002 Effect of preferential concentration on the settling velocity of heavy particles in homogeneous isotropic turbulence. *J. Fluid Mech.* **468**, 77–105.

BEC, J., BIFERALE, L., BOFFETTA, G., CELANI, A., CENCINI, M., LANOTTE, A., MUSACCHIO, S. & TOSCHI, F. 2006 Acceleration statistics of heavy particles in turbulence. *J. Fluid Mech.* **550**, 349–358.

BENZI, R., BIFERALE, L., CALZAVARINI, E., LOHSE, D. & TOSCHI, F. 2009 Velocity-gradient statistics along particle trajectories in turbulent flows: the refined similarity hypothesis in the Lagrangian frame. *Phys. Rev.* E **80** (6), 066318.

BIFERALE, L., SCAGLIARINI, A. & TOSCHI, F. 2010 On the measurement of vortex filament lifetime statistics in turbulence. *Phys. Fluids* **22**, 065101.

BODENSCHATZ, E., MALINOWSKI, S. P., SHAW, R. A. & STRATMANN, F. 2010 Can we understand clouds without turbulence? *Science* **327**, 970–971.

CALZAVARINI, E., VAN DEN BERG, T. H., TOSCHI, F. & LOHSE, D. 2008*a* Quantifying microbubble clustering in turbulent flow from single-point measurements. *Phys. Fluids* **20**, 040702.

CALZAVARINI, E., CENCINI, M., LOHSE, D. & TOSCHI, F. 2008*b* Quantifying turbulence-induced segregation of inertial particles. *Phys. Rev. Lett.* **101**, 084504.

CALZAVARINI, E., KERSCHER, M., LOHSE, D. & TOSCHI, F. 2008*c* Dimensionality and morphology of particle and bubble clusters in turbulent flow. *J. Fluid Mech.* **607**, 13–24.

CHEN, L., GOTO, S. & VASSILICOS, J. C. 2006 Turbulent clustering of stagnation points and inertial particles. *J. Fluid Mech.* **553**, 143–154.

FERENC, J. S. & NÉDA, Z. 2007 On the size distribution of Poisson Voronoï cells. *Physica* A **385**, 518–526.

FESSLER, J. R., KULICK, J. D. & EATON, J. K. 1994 Preferential concentration of heavy particles in a turbulent channel flow. *Phys. Fluids* **6**, 3742–3749.

IJZERMANS, R. H. A., REEKS, M. W., MENEGUZ, E., PICCIOTTO, M. & SOLDATI, A. 2009 Measuring segregation of inertial particles in turbulence by a full Lagrangian approach. *Phys. Rev.* E **80**, 015302(R).

KERSCHER, M., MECKE, K., SCHMALZING, J., BEISBART, C., BUCHERT, T. & WAGNER, H. 2001 Morphological fluctuations of large-scale structure: the PSCz survey. *Astron. Astrophys.* **373**, 1–11.

MARTINEZ MERCADO, J., CHEHATA-GOMEZ, D., VAN GILS, D. P. M., SUN, C. & LOHSE, D. 2010 On bubble clustering and energy spectra in pseudo-turbulence. *J. Fluid Mech.* **650**, 287–306.

MARTINEZ MERCADO, J., PRAKASH, V. N., TAGAWA, Y., SUN, C. & LOHSE, D. 2011 Lagrangian statistics of light particles in turbulence. *Phys. Fluids* (submitted), arXiv:1109.0188v1.

MAXEY, M. R. & RILEY, J. J. 1983 Equation of motion for a small rigid sphere in a non-uniform flow. *Phys. Fluids* **26**, 883–889.

MAZZITELLI, I. M. & LOHSE, D. 2004 Lagrangian statistics for fluid particles and bubbles in turbulence. *New J. Phys.* **6**, 203.

MAZZITELLI, I. M., LOHSE, D. & TOSCHI, F. 2003 On the relevance of the lift force in bubbly turbulence. *J. Fluid Mech.* **488**, 283–313.

MONCHAUX, R., BOURGOIN, M. & CARTELLIER, A. 2010 Preferential concentration of heavy particles: a Voronoï analysis. *Phys. Fluids* **22**, 103304.

OKABE, A., BOOTS, B., SUGIHARA, K. & CHIU, S. N. 2000 *Spatial Tesselations*. Wiley.

PRATSINIS, S. E. & VEMURY, S. 1996 Particle formation in gases: a review. *Powder Technol.* **88**, 267–273.

SAW, E. W., SHAW, R. A., AYYALASOMAYAJULA, S., CHUANG, P. Y. & GYLFASON, A. 2008 Inertial clustering of particles in high-Reynolds-number turbulence. *Phys. Rev. Lett.* **100**, 214501.

SCHMITT, F. G. & SEURONT, L. 2008 Intermittent turbulence and copepod dynamics: increase in encounter rates through preferential concentration. *J. Marine Syst.* **70**, 263–272.

TOSCHI, F., BIFERALE, L., CALZAVARINI, E., SCAGLIARINI, A. & LEVEQUE, E. 2009 Lagrangian modelling and properties of particles with inertia. In *Advances in Turbulence, XII, Proceedings of the 12th European Turbulence Conference (ETC-12), Marburg (D)*, Springer Proceedings in Physics.

TOSCHI, F. & BODENSCHATZ, E. 2009 Lagrangian properties of particles in turbulence. *Annu. Rev. Fluid Mech.* **41**, 375–404.

VAN DE WEYGAERT, R. & ICKE, V. 1989 Fragmenting the universe. Part II. Voronoï vertices as Abell clusters. *Astron. Astrophys.* **213**, 1–9.